Electrical Behavior of Lanthanum Aluminate (LAO) and Gadolinium Doped Ceria (GDG) Composite Electrolyte for Electrochemical Devices

Mohd Najim
Department of Electrical and Electronic Engineering, College of Engineering, University of Jeddah, Saudi Arabia
mngalib@uj.edu.sa
(corresponding author)

Received: 9 November 2022 | Revised: 12 January 2023 | Accepted: 15 January 2023

ABSTRACT

The LAO-GDC solid composite electrolyte has been proposed for use in Solid Oxide Fuel Cells (SOFC). The material conductivity of Solid Carbonate-Ceria (SCC) composite electrolytes is 0.04Scm^{-1} between 400 and 700°C. For this purpose, mixtures of $LaAlO_3$ (LAO) and gadolinium doped ceria $Ce_{0.8}Gd_{0.2}O_2$ (GDC) were created in weight ratios of 3:1, 2:2, and 1:3. The composite electrolyte material was studied separately to improve conductivity. The phase structure and microstructure were studied using an X-Ray Diffractometer (XRD) and Scanning Electron Microscopy (SEM), and the electrical behavior was investigated using Impedance Spectroscopy (IS). The SEM and Energy Dispersive X-ray spectroscopy (EDX) demonstrated a compact structure with an acceptable atomic percentage of constituent elements and a uniform grain distribution. Experimental investigation showed that this composite electrolyte had a high density of $LaAlO_3$ (LAO)-$Ce_{0.8}Gd_{0.2}O_2$ (GDC) composites and an approximate 97% density of its theoretical. The electrical behavior of LAO-GDC composites had the highest value of 0.1Scm^{-1} at 700°C, which is more extreme than the individual conductivities of LAO and GDC, according to Electrochemical Impedance Spectroscopy (EIS) techniques. Among the three composite ratios of the system, only the weight ratio of 3:1 had better conductivity. The $LaAlO_3$ (LAO)-$Ce_{0.8}Gd_{0.2}O_2$ (GDC) composite material has a higher activation energy of 1.5eV.

Keywords-X-Ray Diffractometer (XRD); lanthanum aluminate (LAO); solid electrolyte; electrical conductivity; solid oxide fuel cells (SOFCs)

I. INTRODUCTION

Solid Oxide Fuel Cells (SOFCs) have attracted a lot of attention due to their environmental friendliness, low cost, and lack of possible safety risks [1, 2]. Fuel cell electrolytes are the primary focus of research, since they are the base component of SOFCs. ZrO_2, CeO_2, Bi_2O_3, $LaGaO_3$, and rare earth zirconates are the most widely used solid oxide electrolytes for SOFCs, with Y_2O_3 stabilized ZrO_2 being the most prominent [2-6]. To achieve high electrical conductivity, YSZ requires a high operating temperature of nearly 1000°C. The high operating temperature does not alone pose a significant challenge in terms of electrode selection, however, the cost of materials will rise as a result [4, 7]. The ionic conductivity of YSZ is lower at low temperatures than that of ceria-based electrolytes such as Gadolinium-Doped Ceria (GDC) [8-11]. The conductivity order of both SDC and GDC is around 10^{-2}Scm^{-1} at 750°C, which is comparatively higher than that of stabilized zirconia [12-13]. The closest ionic radius of Gd^{3+} and Ce^{4+} may cause the highest electrical conductivity of GDC [14-15]. In terms of price, processing, and quality, ceria-based electrolytes have been evaluated as a low-temperature alternative. In SOFCs, $LaAlO_3$ may be a good alternative perovskite candidate for the oxide ions conductor (electrolyte) [16-18]. However, in an oxidizing environment, pure $LaAlO_3$ has lower ionic conductivity and more flexible conduction behavior [19]. The ionic conductivity of electrolytes can be best used through composition change by choosing a suitable aliovalent dopant and its optimum concentration [20]. Doping may be uniform or nonuniform depending on whether to form a solid mixture or a composite [21].

This study focused on a composite material as an electrolyte. In general, composite electrolytes are made up of two phases: one that contains regular oxygen ionic conductors and another that contains inorganic salts or oxides. As a result, LAO-GDG is an effective novel electrolyte with a relatively high ionic conductivity at low temperatures [2, 22]. Due to

their high oxygen ion conductivities, doped ceria and lanthanum gallate are investigated as potential ion conductor materials for LT-SOFCs [23-24]. A combination of lanthanum aluminate (LAO) and GDC was recently proposed as a low-cost electrolyte for SOFCs with significantly improved conductivity. In intermediate/low-temperature SOFCs, composite electrolyte materials have been extensively studied for their excellent consistency, electrical conductivity, and thermophysical properties [25-28]. As LAO has a perovskite structure and GDC has a cubic fluorite structure, their combination, perovskite-fluorite, is a great oxide-ion conductor. The GDC-based composite electrolyte material can be prepared using a variety of synthesis methods. In [4], a mechanical mixing process was proposed to create a $GdSmZr_2O_7$-$(Li_{0.52}Na_{0.48})_2CO_3$ composite oxide ion conductor with a conductivity of $0.54Scm^{-1}$ at 600°C, which was substantially higher than that of pure $GdSmZr_2O_7$ [27]. Most studies recorded low sintering temperatures for composites after mixing with an automated ball mill [4]. The sintering temperatures of composite electrolytes have been reported to be lower than those of ancient oxygen-ion ceramics, such as GDC and rare earth zirconates [27-35]. According to [32], a composite electrolyte based on Samarium-Doped Ceria (SDC)–Yttria Stabilized Zirconia (YSZ) exhibits improved electrical conductivity. By molten salt infiltration, a dual composite SDC-LNC was prepared with oxide- and carbonate-ion conductors with a conductivity of $0.46Scm^{-1}$ at 600°C. Coating YSZ with a new composite electrolyte of Yttria Doped Ceria (YDC) and GDC for LT-SOFC was proposed in [33]. Only one cell evaluation revealed that YSZ with doped ceria composite electrolyte, fitted by the sol-gel dip-drawing process, had better cell output than YSZ electrolyte without ceria substrate separation. However, the interdiffusion of constituents at the boundaries can be a disadvantage of YSZ and doped ceria composites, resulting in a decrease in conductivity [21, 34]. It has been discovered that an SDC-LSGM composite electrolyte with a weight ratio of 9:1 has a high oxide ion conductivity [19, 36].

This study investigated the LAO-GDC composite system in terms of phase formation, elemental analysis, and electrical properties. The composites were made using the solid-state reaction process, however, LAO and GDC were prepared and structurally analyzed separately.

II. METHODOLOGY

A solid-state reaction method was adopted to prepare this LAO-GDC-based composite material whereas the LAO was prepared by the auto-combustion method [37]. The following were used to prepare pure LAO, GDC, and the composite material LAO-GDC: $La(NO_3)_3.6H_2O$ (Alfa Aesar, 99%), $Al(NO_3)_3.6H_2O$ (Alfa Aesar, 98%), CeO_2 (99.9%, Sigma Aldrich, USA), and Gd_2O_3 (99.9%, Alfa Aesar, USA). Weighted LAO-GDC composites with LAO:GDC ratios of 3:1, 2:2, and 1:3 were produced. Stoichiometric amounts of LAO and GDC powder substances were mixed by a planetary ball mill using zirconia balls with a diameter of 3mm with ethyl alcohol for 24 hours. After the completion of ball milling, the composite powder was crushed manually in an agate mortar for 4 hours. The residual powder was then calcined at 700°C for 8 hours and then uniaxially pressed into pellets under a pressure of 7 tons ($0.711kg/cm^2$).

The prepared uncured pellets were sintered at a temperature of 1400°C for 12h with a heating-cooling rate of 5°C/min. Sintered pellet XRD patterns were observed using a Rigaku Miniflex II desktop X-ray diffractometer under Cu-Ka radiation (30kV, 20mA) in the 20-80° range. The microstructure of sintered samples was captured using a Quanta 200 FESEM Scanning Electron Microscope (SEM). The existence of critical elements was investigated using Energy-Dispersive X-ray spectroscopy (EDX). The sintered pellets were refined with emery paper to create a clean and smooth surface layer, and then silver (Ag) paste was pasted on both sides of the pellet and fired for half an hour at 700°C. The electrical behavior of these pellets was studied using a Wayne Kerr 6500 P impedance analyzer in the range of 400-700°C at a step of 25°C in the frequency range of 20Hz to 1MHz. Based on Archimedes' theory, the experimental densities of prepared sintered pellets were calculated using a density measurement instrument (Sartorius, BSA2245CW).

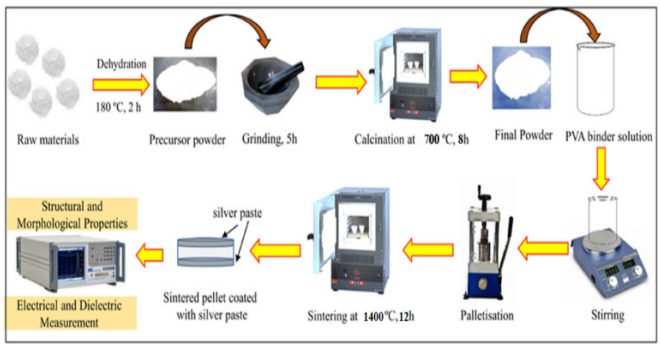

Fig. 1. Solid-state reaction synthesis techniques

III. RESULTS AND DISCUSSION

This study investigated LAO-GDC with weight ratios of 3:1, 2:2, and 1:3, called L3G1, L2G2, and L1G3, respectively.

A. Structural and Morphological Properties

Figure 2(a) shows the XRD patterns of all the LAO-GDC structures investigated, and the composites L3G1, L2G2, and L1G3. LAO and GDC phases are represented by the symbols ♦ and *, respectively, and the phases of all explored system components are also indicated. The expanded view shown in Figure 2(b) of the more intense peak between 20-35°C clearly shows the minor right shifting of the peaks as the GDC doping concentration increased. The intensity of the peak corresponding to a 121 plane decreases with increasing GDC concentration, showing decreasing crystallite size in the SEM micrograph. The XRD phase patterns of LAO and GDC are also listed as references, with single-phase rhombohedral perovskite structure and cubic fluorite structure, respectively, having space groups R-3c and Fm3m that suit well with the JCPDS files no. 82-0478 and 81-0792. The system shows single-phase formation as a result of high-temperature sintered pellets. This study achieved an optimized conductivity of $0.46\times10^{-1}Scm^{-1}$ for the L1G3 system; therefore, the physical behavior of this composite is discussed.

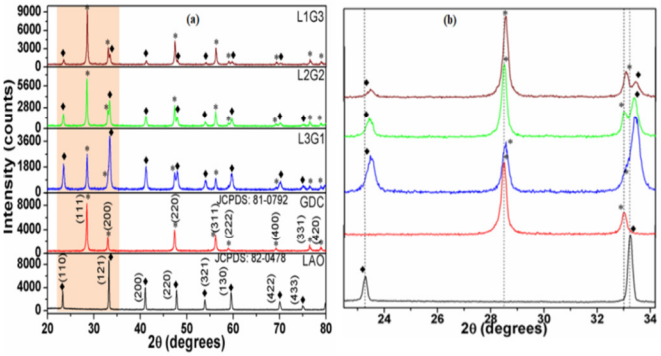

Fig. 2. (a) XRD pattern of LAO, GDC, and their composites L3G1, L2G2, and L1G3, (b) expanded view of the more intense peak between 20-35°C (crystal structure).

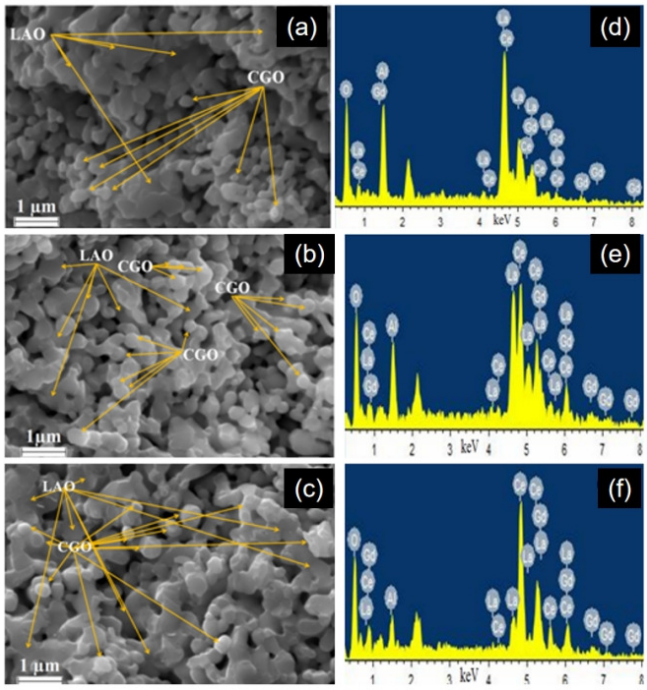

Fig. 3. SEM Microstructure of composites (a) L3G1, (b) L2G2, and (c) L1G3. Elemental mapping of composites: (d) L3G1, (e) L2G2, and (f) L1G3.

The XRD pattern of sintered composite pellets consists of perovskite rhombohedral structure (R-3c) LAO as a major phase along with minor GDC cubic fluorite structure (space group, Fm3m). Peaks were indexed using the above-mentioned space group [16, 38]. Using the Archimedes principle, the densities of sintered composite pellets were measured at 6.4, 6.6, and 6.7g/cm^2 for L3G1, L2G2, and L1G3, respectively, which is 97% of the theoretically calculated va;ues. The SEM micrographs of the sintered pellets' rupture surface were logged for all systems. Figure 3 illustrates the SEM micrograph of the fractured samples of all three composites. The SEM image clearly shows hexagonal and cubic grains having dense and well-connected structures. The SEM micrographs clearly show the white color cubic structure of the GDC and are in good agreement with XRD patterns. The captured SEM microstructure shows a very dense and compact shape for L1G3 than the others, which is congruent with observed experimental density values. Furthermore, SEM micrographs depict comparatively small grain sizes when increasing the GDC ratio. The average particle size of all three compositions was calculated using the linear intercept process, yielding values in the range of 1.27-1.98nm. The average grain size value for L1G3 was found to be lower than those of the other compositions. Using Scherer's formula, the average crystallite size was calculated to be in the 40-50nm range [16]. The structure with a smaller particle size or a large grain boundary has more oxygen vacancies resulting in higher conductivity [13, 19, 38]. The Energy-Dispersive Spectroscopy (EDS) study, shown in Figure 4, shows all the atomic constituents and their atomic percentage. The percentage of the atomic value of O, Ce, and Gd is higher in L1G3. The elemental mapping (Figure (3 (d-f)) for all composite systems showed the presence of all elements in their appropriate ratio which is also confirmed by the EDX study in Figure 4.

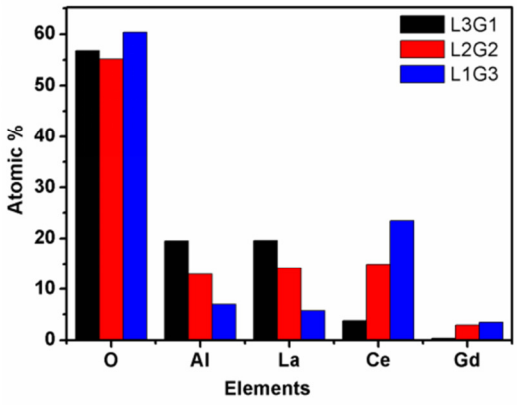

Fig. 4. EDS of the composites L3G1, L2G2, and L1G3.

B. Electrical Properties

The electrical behavior of composites was studied using complex plane impedance analysis in the frequency range of 20Hz to 1MHz. Two constraints were used to estimate the electrical conductivity: conductance (G) and dielectric constant (D). The real (Z') and the imaginary (Z'') part of impedance were used in the complex plane impedance analysis [16] and can be calculated with the help of the formula given in (1) and plotted on the x and y axes, respectively.

$$Z' = \frac{D^2}{G(D^2+1)} \quad \text{and} \quad Z'' = \frac{Z'}{D} \tag{1}$$

Figure 5 shows the representative Nyquist graph of the L1G3 composite in different temperature ranges of 475-700°C. Complete conductivity is the sum of all individual conductivities attributable to the grain, grain boundary, and electrode-specimen interface in high-, intermediate-, and low-frequency regions, respectively [34, 39-40]. A wide semicircular arc near the origin was observed at low temperatures (400°C), indicating a high-frequency field, due to grain influence.

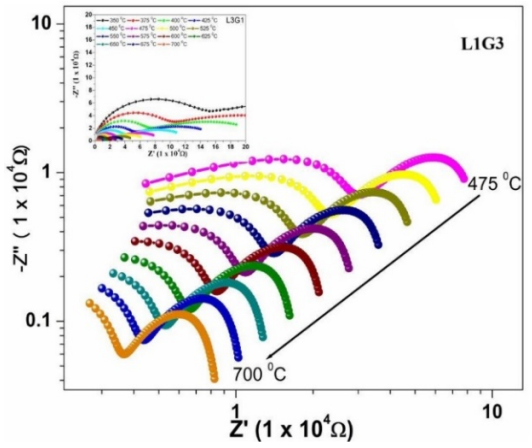

Fig. 5. Nyquist plots of L3G1 composite in the temperature range of 475-700°C.

Increasing temperature, this large semicircular curve due to grain contribution (near the origin) becomes small at intermediate temperatures and disappears at high temperatures. This movement of the semicircular arc to the right-hand side is due to the relaxation frequency of polarization processes [34, 39-41]. Therefore, with increasing temperature, the semicircular arc related to grain contribution disappears, as shown in Figures 5 and 6 (the latter being plotted in log scale). The semicircular arc due to electrode polarization starts to appear at a high temperature and is visible at ~700°C. At high temperatures (700°C), at first the straight line due to the grain contribution appears, and then the single semicircle, as shown in Figure 6(b), at the in-between frequency indicates that conduction is primarily through grain boundaries [39-42]. Since the ratio of grain boundary resistance (Rgb) to grain resistance (R_g) is not important, grains play a significant role in total conductivity at low temperatures, i.e. $R_{gb}<R_g$. However, on increasing temperatures, this ratio increases slowly and becomes large at high temperatures (~700°C), i.e. $R_{gb}>R_g$. Finally, at 700°C and above, the grain resistance (Rg) vanishes, and the overall conductivity of the sample is calculated by the grain boundary resistance (R_{gb}). As a result, at high temperatures, the conductivity due to grain boundary influences conductivity due to the grain (~700°C). The grain resistance (R_g) and grain boundaries resistances (R_{gb}) can be calculated by calculating the intercepts of respective arcs on the real axis (Z').

Temperature dependence activation energy for the composite L1G3 is exposed by the Arrhenius plot with log (σT) on the y-axis vs 1000/T on the x-axis, as shown in Figure 5. A linear relationship (straight line) was observed in the complete temperature range (400-700°C). The activation energy (E_a) of the composite L1G3 is determined by the slope of this straight line, as shown in Figure 5. The formation energy and migration barrier may be triggering the activation energy for conduction. The conductivity of a material is related to the defect and is measured as $\sigma=ne\mu$, where n, e, and μ are the concentration, the charge of the defect, and the mobility, respectively. The concentration n, on the other hand, consists of both thermally activated and athermal defects [41], i.e., $n=n_a+n_t$, where n_t is the concentration of defects that are thermally stimulated in the measurements at predetermined temperatures and n_a is the athermal concentration involving defects, e.g. prior in the material before the conductivity measurements but at lower temperatures. This study measured samples at intermediate temperatures from 400 to 700°C and therefore the thermally activated defects play an important role, i.e. $n_t>n_a$. Furthermore, since $E_a=E_f+E_m$ [41], the measured value of the activation energies (E_a) was found to be approximately 1.5eV, which is in good agreement with the values of LAO and GDC in [20, 43], and indicates that the activation energy of ionic conduction is comparable to the activation energy of vacancy mobility [19]. The mobility of oxygen ions is a temperature-dependent property that decreases as the temperature increases [44-45]. Equation (2) can be used to express the temperature-dependent ionic conductivity:

$$\sigma = \sigma_o \exp(\frac{-E_a}{K_B T}) \quad (2)$$

where σ_0 is a fixed exponent factor and reverse temperature dependent. The measured activation energy values reveal that the movement of oxide ions is caused by ionic transport [20, 44, 46].

The activation energy of an electrolyte device (oxide ion conductor) is estimated to range between 0.9 and 1.8eV [20, 47, 49-50]. Therefore, the investigated composite system is ionic in nature, and its conductivity is mainly determined by thermally activated oxygen ions [49-51]. The ionic conductivity of all investigated compositions, at 700°C, was found to be of the order of 10^{-1}Scm^{-1} and L1G3 showed the highest conductivity magnitude. The ionic conductivity was found to be related to the development of oxygen vacancies at high temperatures. The conductivity of the investigated LAO-GDC composite systems increases as the GDC ratio increases due to the formation of oxygen ion vacancies, which are primarily formed by Gd^{3+} ions. Consequently, dopant concentration, grain boundaries, and grain size play an important role in determining conductivity and its variation.

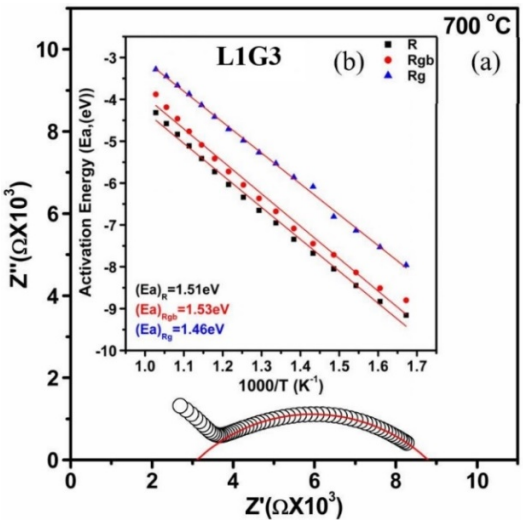

Fig. 6. (a) Representative fitted Nyquist plot of L1G3 at 700°C, (b) Arrhenius representation of conductivity of L1G3 at different temperatures (insight).

The influence of Gd^{3+} ions on the lanthanum site plays a role when the conductivity is rising and then falls off activation energy accordingly. The activation energy of pure $LaAlO_3$ was reported as 0.90±0.01eV [52], while the activation energy of GDC was reported as 0.55-1.04eV [11, 14] and for the LAO-GDC composites was found to be 1.51eV. The value of the observed activation energy for this composite shows enhanced ionic conductivity which rises with a rise in the GDC ratio. Furthermore, the improvement in conductivity is consistent with the compact microstructure of the composites. The conductivity of the L1G3 composition was found to be the highest among the three compositions investigated and provides a better option for cost-effective solid electrolyte applications in electrochemical devices.

IV. DISCUSSION

At moderate temperatures, the conductivities of GDC are approximately $10^{-2}Scm^{-1}$, which is inflated when compared to stabilized zirconia. The maximum electrical conductivity of GDC may be a result of the fact that Gd^{3+} and Ce^{4+} have close ionic radii. Ceria-based electrolytes have been examined as a low-temperature alternative in terms of cost, processing, and quality. $LaAlO_3$ might be a good substitute perovskite option for the oxide ion conductor in SOFCs. Improved electrical conductivity can be found in a composite electrolyte made of Samarium-Doped Ceria (SDC) and Yttria Stabilized Zirconia (YSZ).

In this paper, a dual composite SDC-LNC constructed with oxide- and carbonate-ion conductors with a conductivity of $0.46Scm^{-1}$ at 600°C was infiltrated with molten salt. Cell evaluation showed that the sol-gel dip-drawing procedure fitted YSZ with a doped ceria composite electrolyte had better cell output than the YSZ electrolyte without ceria substrate separation. However, YSZ and doped ceria composites may suffer from the inter-diffusion of components at the borders, which would reduce conductivity. An SDC-LSGM composite electrolyte with a weight ratio of 9:1 has previously been found to have a high oxide ion conductivity.

V. CONCLUSION

This study successfully synthesized LAO-GDC composites employing a quick, simple, and efficient solid-state reaction method, with typical crystallite sizes of 41-50nm. LAO and GDC, respectively, made the hexagonal and cubic fluorite structures visible. When these two were joined, LAO-GDC composites showed the same phase. The density of the high-density composite systems sintered at 1400°C was 97% of the theoretical. The L1G3 samples had a microstructure that is more dense and fine than the other samples. As the amount of Gd^{3+} doping was increased, GDC's conductivity rose. The L1G3 composition obtained its maximum conductivity of $0.4\times10^{-1}Scm^{-1}$ with an activation energy of 1.51eV. The LAO-GDC composite is predominantly an L1G3 system, as seen by this peculiar electrical behavior.

ACKNOWLEDGMENT

This work was funded by the Deanship of Scientific Research (DSR), University of Jeddah, Saudi Arabia, under Grant No. UJ-20-006-DR. Therefore, the author acknowledges the University for the technical and financial support. The author is also grateful to the Indian Institute of Technology in Kanpur, for providing the experimental facilities.

REFERENCES

[1] S. A. Saadabadi, A. Thallam Thattai, L. Fan, R. E. F. Lindeboom, H. Spanjers, and P. V. Aravind, "Solid Oxide Fuel Cells fuelled with biogas: Potential and constraints," *Renewable Energy*, vol. 134, pp. 194–214, Apr. 2019, https://doi.org/10.1016/j.renene.2018.11.028.

[2] B. Singh, S. Ghosh, S. Aich, and B. Roy, "Low temperature solid oxide electrolytes (LT-SOE): A review," *Journal of Power Sources*, vol. 339, pp. 103–135, Jan. 2017, https://doi.org/10.1016/j.jpowsour.2016.11.019.

[3] J. Patakangas, Y. Ma, Y. Jing, and P. Lund, "Review and analysis of characterization methods and ionic conductivities for low-temperature solid oxide fuel cells (LT-SOFC)," *Journal of Power Sources*, vol. 263, pp. 315–331, Oct. 2014, https://doi.org/10.1016/j.jpowsour.2014.04.008.

[4] Y. J. Jin, Z. G. Liu, Z. Y. Ding, G. Cao, and J. H. Ouyang, "Preparation, microstructure and electrical property of GdSmZr2O7-(Li0.52Na0.48)2CO3 composite electrolyte via carbonate infiltration," *Ceramics International*, vol. 46, no. 5, pp. 5689–5694, Apr. 2020, https://doi.org/10.1016/j.ceramint.2019.11.016.

[5] Raghvendra, R. K. Singh, and P. Singh, "Electrical conductivity of LSGM–YSZ composite materials synthesized via coprecipitation route," *Journal of Materials Science*, vol. 49, no. 16, pp. 5571–5578, Aug. 2014, https://doi.org/10.1007/s10853-014-8265-5.

[6] Z. Wang, Y. Zeng, C. Li, Z. Ye, L. Cao, and Y. Zhang, "Structures and electrical conductivities of Gd3+ and Fe3+ co-doped cerium oxide electrolytes sintered at low temperature for ILT-SOFCs," *Ceramics International*, vol. 44, no. 9, pp. 10328–10334, Jun. 2018, https://doi.org/10.1016/j.ceramint.2018.03.041.

[7] L. Carrette, K. A. Friedrich, and U. Stimming, "Fuel cells - fundamentals and applications," *Fuel Cells*, vol. 1, May 2001, https://doi.org/10.1002/1615-6854(200105)1:1<5::AID-FUCE5>3.0.CO;2-G.

[8] İ. Ermiş and S. P. S. Shaikh, "Study of crystallographic, thermal and electrical properties of (Bi2O3)1-x-y(Tb4O7)x(Gd2O3)y electrolyte for SOFC application," *Ceramics International*, vol. 44, no. 15, pp. 18776–18782, Oct. 2018, https://doi.org/10.1016/j.ceramint.2018.07.109.

[9] S. P. S. Badwal and K. Foger, "Solid oxide electrolyte fuel cell review," *Ceramics International*, vol. 22, no. 3, pp. 257–265, Jan. 1996, https://doi.org/10.1016/0272-8842(95)00101-8.

[10] J. B. Goodenough, A. Manthiram, M. Paranthaman, and Y. S. Zhen, "Oxide ion electrolytes," *Materials Science and Engineering: B*, vol. 12, no. 4, pp. 357–364, Feb. 1992, https://doi.org/10.1016/0921-5107(92)90006-U.

[11] S. (Rob) Hui *et al.*, "A brief review of the ionic conductivity enhancement for selected oxide electrolytes," *Journal of Power Sources*, vol. 172, no. 2, pp. 493–502, Oct. 2007, https://doi.org/10.1016/j.jpowsour.2007.07.071.

[12] A. B. Stambouli and E. Traversa, "Solid oxide fuel cells (SOFCs): a review of an environmentally clean and efficient source of energy," *Renewable and Sustainable Energy Reviews*, vol. 6, no. 5, pp. 433–455, Oct. 2002, https://doi.org/10.1016/S1364-0321(02)00014-X.

[13] N. K. Singh, P. Singh, M. K. Singh, D. Kumar, and O. Parkash, "Auto-combustion synthesis and properties of Ce0.85Gd0.15O1.925 for intermediate temperature solid oxide fuel cells electrolyte," *Solid State Ionics*, vol. 192, no. 1, pp. 431–434, Jun. 2011, https://doi.org/10.1016/j.ssi.2010.04.015.

[14] T. Kudo and H. Obayashi, "Oxygen Ion Conduction of the Fluorite-Type Ce1 − x Ln x O 2 − x / 2 (Ln = Lanthanoid Element)," *Journal of The Electrochemical Society*, vol. 122, no. 1, Jan. 1975, Art. no. 142, https://doi.org/10.1149/1.2134143.

[15] N. Jaiswal, N. K. Singh, D. Kumar, and O. Parkash, "Effect of strontium (Sr) doping on the conductivity of ceria," *Journal of Power Sources*, vol. 202, pp. 78–84, Mar. 2012, https://doi.org/10.1016/j.jpowsour.2011.10.140.

[16] X. Li, Z. Feng, J. Lu, F. Wang, M. Xue, and G. Shao, "Synthesis and electrical properties of Ce1−xGdxO2−x/2 (x=0.05–0.3) solid solutions prepared by a citrate–nitrate combustion method," *Ceramics International*, vol. 38, no. 4, pp. 3203–3207, May 2012, https://doi.org/10.1016/j.ceramint.2011.12.025.

[17] R. V. Mangalaraja *et al.*, "Electrical and thermal characterization of Sm3+ doped ceria electrolytes synthesized by combustion technique," *Journal of Alloys and Compounds*, vol. 510, no. 1, pp. 134–140, Jan. 2012, https://doi.org/10.1016/j.jallcom.2011.09.016.

[18] O. N. Verma, S. Singh, V. K. Singh, M. Najim, R. Pandey, and P. Singh, "Influence of Ba Doping on the Electrical Behaviour of La0.9Sr0.1Al0.9Mg0.1O3−δ System for a Solid Electrolyte," *Journal of Electronic Materials*, vol. 50, no. 3, pp. 1010–1021, Mar. 2021, https://doi.org/10.1007/s11664-020-08653-2.

[19] O. N. Verma, N. K. Singh, Raghvendra, and P. Singh, "Study of ion dynamics in lanthanum aluminate probed by conductivity spectroscopy," *RSC Advances*, vol. 5, no. 28, pp. 21614–21619, Feb. 2015, https://doi.org/10.1039/C5RA01146A.

[20] L. John Berchmans, S. Angappan, A. Visuvasam, and K. B. Ranjith Kumar, "Preparation and characterization of LaAlO3," *Materials Chemistry and Physics*, vol. 109, no. 1, pp. 113–118, May 2008, https://doi.org/10.1016/j.matchemphys.2007.11.007.

[21] T. L. Nguyen, M. Dokiya, S. Wang, H. Tagawa, and T. Hashimoto, "The effect of oxygen vacancy on the oxide ion mobility in LaAlO3-based oxides," *Solid State Ionics*, vol. 130, no. 3, pp. 229–241, May 2000, https://doi.org/10.1016/S0167-2738(00)00640-8.

[22] O. N. Verma, P. K. Jha, and P. Singh, "A structural–electrical property correlation in A-site double substituted lanthanum aluminate," *Journal of Applied Physics*, vol. 122, no. 22, Dec. 2017, Art. no. 225106, https://doi.org/10.1063/1.4999002.

[23] W. S. Jang, S. H. Hyun, and S. G. Kim, "Preparation of YSZ/YDC and YSZ/GDC composite electrolytes by the tape casting and sol-gel dip-drawing coating method for low-temperature SOFC," *Journal of Materials Science*, vol. 37, no. 12, pp. 2535–2541, Jun. 2002, https://doi.org/10.1023/A:1015451910081.

[24] J. H. Kim, Y. Kim, P. A. Connor, J. T. S. Irvine, J. Bae, and W. Zhou, "Structural, thermal and electrochemical properties of layered perovskite SmBaCo2O5+d, a potential cathode material for intermediate-temperature solid oxide fuel cells," *Journal of Power Sources*, vol. 194, no. 2, pp. 704–711, Dec. 2009, https://doi.org/10.1016/j.jpowsour.2009.06.024.

[25] J. Huang, Z. Mao, L. Yang, and R. Peng, "SDC-Carbonate Composite Electrolytes for Low-Temperature SOFCs," *Electrochemical and Solid-State Letters*, vol. 8, no. 9, Jul. 2005, Art. no. A437, https://doi.org/10.1149/1.1960139.

[26] T. Fukui, S. Ohara, Kenji. Murata, H. Yoshida, K. Miura, and T. Inagaki, "Performance of intermediate temperature solid oxide fuel cells with La(Sr)Ga(Mg)O3 electrolyte film," *Journal of Power Sources*, vol. 106, no. 1, pp. 142–145, Apr. 2002, https://doi.org/10.1016/S0378-7753(01)01026-6.

[27] W. Sun, M. Liu, and W. Liu, "Chemically Stable Yttrium and Tin Co-Doped Barium Zirconate Electrolyte for Next Generation High Performance Proton-Conducting Solid Oxide Fuel Cells," *Advanced Energy Materials*, vol. 3, no. 8, pp. 1041–1050, 2013, https://doi.org/10.1002/aenm.201201062.

[28] A. J. Abd Aziz, N. A. Baharuddin, M. R. Somalu, and A. Muchtar, "Review of composite cathodes for intermediate-temperature solid oxide fuel cell applications," *Ceramics International*, vol. 46, no. 15, pp. 23314–23325, Oct. 2020, https://doi.org/10.1016/j.ceramint.2020.06.176.

[29] L. Fan*, "Solid-State Electrolytes for SOFC," in *Solid Oxide Fuel Cells*, John Wiley & Sons, Ltd, 2020, pp. 35–78.

[30] C. Salvo, R. V. Mangalaraja, R. Udayabashkar, M. Lopez, and C. Aguilar, "Enhanced mechanical and electrical properties of novel graphene reinforced copper matrix composites," *Journal of Alloys and Compounds*, vol. 777, pp. 309–316, Mar. 2019, https://doi.org/10.1016/j.jallcom.2018.10.357.

[31] S. Dwivedi, "Solid oxide fuel cell: Materials for anode, cathode and electrolyte," *International Journal of Hydrogen Energy*, vol. 45, no. 44, pp. 23988–24013, Sep. 2020, https://doi.org/10.1016/j.ijhydene.2019.11.234.

[32] Y. Mishima, H. Mitsuyasu, M. Ohtaki, and K. Eguchi, "Solid Oxide Fuel Cell with Composite Electrolyte Consisting of Samaria-Doped Ceria and Yttria-Stabilized Zirconia," *Journal of The Electrochemical Society*, vol. 145, no. 3, Mar. 1998, Art. no. 1004, https://doi.org/10.1149/1.1838378.

[33] L. Zhang, X. Li, S. Wang, K. G. Romito, and K. Huang, "High conductivity mixed oxide-ion and carbonate-ion conductors supported by a prefabricated porous solid-oxide matrix," *Electrochemistry Communications*, vol. 13, no. 6, pp. 554–557, Jun. 2011, https://doi.org/10.1016/j.elecom.2011.03.008.

[34] N. Mahato, A. Gupta, and K. Balani, "Doped zirconia and ceria-based electrolytes for solid oxide fuel cells: a review," *Nanomaterials and Energy*, vol. 1, no. 1, pp. 27–45, Jan. 2012, https://doi.org/10.1680/nme.11.00004.

[35] C. Papadakis, Y. Yin, M. Danikas, and C. Charalambous, "Surface Discharges and Flashover Voltages in Nanocomposite XLPE Samples," *Engineering, Technology & Applied Science Research*, vol. 8, no. 6, pp. 3502–3504, Dec. 2018, https://doi.org/10.48084/etasr.2186.

[36] P. Löfkvist, "Fabrication of a light-weight SOFC using ceramic fibre paper as substrate," MSc Thesis, Lund University, Lund, Sweden, 2015.

[37] D. Xu *et al.*, "Fabrication and characterization of SDC–LSGM composite electrolytes material in IT-SOFCs," *Journal of Alloys and Compounds*, vol. 429, no. 1, pp. 292–295, Feb. 2007, https://doi.org/10.1016/j.jallcom.2006.04.009.

[38] B. Li, S. Liu, X. Liu, G. Hao, H. Wang, and W. Su, "Study on GDC-LSGM composite electrolytes for intermediate-temperature solid oxide fuel cells," *International Journal of Hydrogen Energy*, vol. 38, no. 26, pp. 11392–11397, Aug. 2013, https://doi.org/10.1016/j.ijhydene.2013.06.116.

[39] A. Tschöpe, E. Sommer, and R. Birringer, "Grain size-dependent electrical conductivity of polycrystalline cerium oxide: I. Experiments," *Solid State Ionics*, vol. 139, no. 3, pp. 255–265, Feb. 2001, https://doi.org/10.1016/S0167-2738(01)00678-6.

[40] A. Tschöpe, "Grain size-dependent electrical conductivity of polycrystalline cerium oxide II: Space charge model," *Solid State Ionics*, vol. 139, no. 3, pp. 267–280, Feb. 2001, https://doi.org/10.1016/S0167-2738(01)00677-4.

[41] S. U. Sharath, R. K. Singh, Raghvendra, B. P. Singh, P. Kumar, and P. Singh, "Influence of Grain and Grain-Boundary Resistances on Dielectric Properties of KNbO3 Under Small DC Bias Field," *Journal of the American Ceramic Society*, vol. 96, no. 10, pp. 3127–3132, 2013, https://doi.org/10.1111/jace.12466.

[42] A. P. Sakhya, A. Dutta, and T. P. Sinha, "Dielectric relaxation of samarium aluminate," *Applied Physics A*, vol. 114, no. 4, pp. 1097–1104, Mar. 2014, https://doi.org/10.1007/s00339-013-7766-4.

[43] T. Lan Nguyen and M. Dokiya, "Electrical conductivity, thermal expansion and reaction of (La, Sr)(Ga, Mg)O3 and (La, Sr)AlO3 system," *Solid State Ionics*, vol. 132, no. 3, pp. 217–226, Jul. 2000, https://doi.org/10.1016/S0167-2738(00)00661-5.

[44] K. Hoang, M. Oh, and Y. Choi, "Electronic Structure and Properties of Lithium-Rich Complex Oxides," *ACS Applied Electronic Materials*, vol. 1, no. 1, pp. 75–81, Jan. 2019, https://doi.org/10.1021/acsaelm.8b00025.

[45] D. Lybye, F. W. Poulsen, and M. Mogensen, "Conductivity of A- and B-site doped LaAlO3, LaGaO3, LaScO3 and LaInO3 perovskites," *Solid State Ionics*, vol. 128, no. 1, pp. 91–103, Feb. 2000, https://doi.org/10.1016/S0167-2738(99)00337-9.

[46] J. Y. Park and G. M. Choi, "Electrical conductivity of Sr and Mg doped LaAlO3," *Solid State Ionics*, vol. 154–155, pp. 535–540, Dec. 2002, https://doi.org/10.1016/S0167-2738(02)00510-6.

[47] D. Aroussi, B. Aour, and A. S. Bouaziz, "A Comparative Study of 316L Stainless Steel and a Titanium Alloy in an Aggressive Biological Medium," *Engineering, Technology & Applied Science Research*, vol. 9, no. 6, pp. 5093–5098, Dec. 2019, https://doi.org/10.48084/etasr.3208.

[48] M. V. Japitana and M. E. C. Burce, "A Satellite-based Remote Sensing Technique for Surface Water Quality Estimation," *Engineering, Technology & Applied Science Research*, vol. 9, no. 2, pp. 3965–3970, Apr. 2019, https://doi.org/10.48084/etasr.2664.

[49] H. Hayashi, H. Inaba, M. Matsuyama, N. G. Lan, M. Dokiya, and H. Tagawa, "Structural consideration on the ionic conductivity of perovskite-type oxides," *Solid State Ionics*, vol. 122, no. 1, pp. 1–15, Jul. 1999, https://doi.org/10.1016/S0167-2738(99)00066-1.

[50] M. A. Biberci and M. B. Celik, "Dynamic Modeling and Simulation of a PEM Fuel Cell (PEMFC) during an Automotive Vehicle's Driving Cycle," *Engineering, Technology & Applied Science Research*, vol. 10, no. 3, pp. 5796–5802, Jun. 2020, https://doi.org/10.48084/etasr.3352.

[51] K. Hoang, "First-principles theory of doping in layered oxide electrode materials," *Physical Review Materials*, vol. 1, no. 7, Dec. 2017, Art. no. 075403, https://doi.org/10.1103/PhysRevMaterials.1.075403.

[52] H. J. Park and G. M. Choi, "Oxygen permeation in Sr- and Mg-doped LaAlO3 and Gd-doped CeO2 at high temperature," *Solid State Ionics*, vol. 175, no. 1, pp. 399–403, Nov. 2004, https://doi.org/10.1016/j.ssi.2004.03.048.